Hydrogen Evolving Activity of Dithiolene-Based Metal-Organic Frameworks with Mixed Cobalt and Iron Centers

Keying Chen[‡], Courtney A. Downes[‡], Jason D. Goodpaster[§], and Smaranda C. Marinescu*[‡]

‡Department of Chemistry, University of Southern California, Los Angeles, California 90089, United States.

§Department of Chemistry, University of Minnesota – Twin Cities, Minneapolis, Minnesota 55455, United States

KEYWORDS Metal dithiolene, metal-organic framework, electrocatalysis, hydrogen evolution

ABSTRACT: Electrocatalytic systems based on metal-organic frameworks (MOFs) have attracted great attention due to their potential application in commercially viable renewable energy-converting devices. We have recently shown that the cobalt 2,3,6,7,10,11-triphenylenehexathiolate (**CoTHT**) framework can catalyze the hydrogen evolution reaction (HER) in fully aqueous media with Tafel slopes as low as 71 mV/dec and near unity Faradaic efficiency (FE). Taking advantage of the high synthetic tunability of MOFs, here we synthesize a series of iron and mixed iron/cobalt THT-based MOFs. The incorporation of the iron and cobalt dithiolene moieties is verified by various spectroscopic techniques, and the integrity of the crystalline structure is maintained regardless of the stoichiometries of the two metals. The hydrogen evolving activity of the materials was explored in pH 1.3 aqueous electrolyte solutions. Unlike **CoTHT**, the **FeTHT** framework exhibits minimal activity due to a late catalytic onset (-0.440 V versus RHE) and a large Tafel slope (210 mV/dec). The performance of the mixed-metal MOFs is adversely affected by the incorporation of Fe, where increasing Fe content results in MOFs with lower HER activity and diminished long-term stability and FE for H_2 production. It is proposed that the **FeTHT** domains undergo alternative Faradaic processes under catalytic conditions, which alter its local structure and electrochemical behavior, eventually resulting in a material with diminished HER performance.

INTRODUCTION

Metal-organic frameworks (MOFs) have attracted growing attention as a new class of functional materials over the last two decades. Their unique properties, such as large surface area, permanent porosity, structural regularity, and high synthetic tunability, endow MOFs with potential for a wide spectrum of applications.[1] In the context of increased global energy consumption and environmental issues, the development of MOF-based electrocatalysts has become an emerging research topic in recent years.[2] The rigid structure and hybrid nature of MOFs make them an excellent platform for the heterogenization of molecular catalysts, a novel strategy to construct catalytic materials with improved stability and reusability.[2,3] More importantly, this strategy allows for the understanding and optimization of the activity of a bulk material at the molecular level. To date, many MOF-based electrocatalytic systems have been reported for various reactions, including the hydrogen evolution reaction (HER),[4–14] oxygen evolution reaction (OER),[15–20] oxygen reduction reaction (ORR),[21–26] and CO_2 reduction (CO_2RR).[27–33]

Dithiolene-based MOFs are among the most active MOFs for electrocatalytic HER.[4–9,14,34] This class of 2D MOFs are typically constructed by linking single-metal centers with trinucleating ligands such as benzenehexathiolate (BHT) and triphenylene-2,3,6,7,10,11-hexathiolate (THT). MOFs incorporating cobalt or nickel as active metal centers have been extensively studied for the HER,[5,7,9] with **CoTHT** displaying the lowest overpotential (143 mV) to reach the benchmarking metric of 10 mA/cm^2, a Tafel slope of only 71 mV/dec, and with near unity Faradaic efficiency (FE) for H_2 evolution.[4] However, the electrocatalytic activity of the iron dithiolene-based MOFs remains relatively unexplored. The molecular iron dithiolene complexes have been shown to exhibit moderate activity towards visible-light-driven photocatalytic HER with high turnover numbers in conjunction with CdSe quantum dots as a photosensitizer and ascorbic acid as the electron donor.[35] Additionally, prior report has suggested that the iron dithiolene coordination polymer based on the BHT ligand (**FeBHT**) was capable of performing HER with decent activity, characterized by a Tafel slope of 119 mV/dec and an overpotential of 473 mV to reach 10 mA/cm^2 in fully aqueous mdia.[8] Although the electrocatalytic activity of **FeTHT** has not been reported, recent studies regarding its physical properties have suggested that **FeTHT** films exhibit similar room-temperature electrical conductivity compared to that of the **CoTHT** films, with values ranging between 0.02 and 0.3 S·cm^{-1}.[36,37] The room-temperature mobility of **FeTHT** was reported to be ~220 cm^{2}V^{-1}s^{-1}, a record high value for MOFs.[38] Based on these previous studies and the fact that iron is inexpensive and more abundant than cobalt, the investigation of the HER performance of **FeTHT** is of great interest.

The hybrid nature of MOFs allows for a high degree of variability and multivariate synthetic tunability. Such tunability has been explicitly studied by Yaghi and coworkers where MOFs were shown to incorporate up to 8 unique ligands and 10 different metals without disturbing the crystalline structure of the overall framework.[39,40] In the context of electrocatalysis, introducing multiple metal centers into the same structure is a

common strategy to improve the catalytic performance.[41–43] For example, it is well-known that the incorporation of Fe into Co or Ni (oxy)hydroxides can dramatically improve the OER performance of the catalysts.[44,45] Chang and coworkers also reported the synthesis of the multivariate Co/Cu COF-367 for CO_2 reduction. The incorporation of Cu allowed for dilution of the active Co sites and substantially enhanced activity on a per-cobalt basis.[29] Hence, we sought to utilize the high synthetic tunability of MOFs to design a series of mixed Co/Fe MOF electrocatalysts and investigate the influence of different metal moieties on the HER activity.

Herein, a series of dithiolene-based MOFs incorporating Co and Fe metal centers with variable ratios were successfully synthesized and characterized. The presence of both metals was analyzed by various spectroscopic techniques. The electrocatalytic HER activity of the materials was studied in pH 1.3 aqueous solutions. It is found that, unlike its cobalt analogue, **FeTHT** exhibits minimal activity towards the HER. More interestingly, the incorporation of the Fe centers also drastically reduces the activity and stability of the mixed-metal frameworks. It is proposed that the **FeTHT** undergoes alternative Faradaic processes under catalytic conditions, which alter its local structure and electrochemical behavior, resulting in a material with diminished activity for the HER.

RESULTS AND DISCUSSION

Synthesis and Characterization. Prior reports have suggested that both **CoTHT** and **FeTHT** can be synthesized through the liquid-liquid interfacial synthesis, which was proposed to lead to materials with high structural similarity.[5,36,37] Therefore, it was expected that similar synthetic methodology would be applicable to the mixed-metal MOFs. To tune the stoichiometries of the metals in the resulting MOFs, metal precursors were prepared as a series of solutions of $CoCl_2$ and $FeCl_2$ with different molar ratios and underwent similar liquid-liquid interfacial synthetic procedure (see SI for experimental details). The resulting mixed-metal frameworks (**CoFeTHT**) were collected as powder, solvent exchanged with water (3×) and methanol (3×), then dried under vacuum. We confirmed the incorporation and determined the concentration of each metal within the frameworks by inductively coupled plasma optical emission spectroscopy (ICP-OES) measurements with results summarized in Table 1. Analysis by ICP-OES reveals that both Co and Fe are successfully incorporated into the framework through this synthetic method. Additionally, altering the feeding molar ratios of the precursors results in MOFs with varied metal compositions, and such variability is relatively reproducible by comparing the composition of the materials prepared from three individual trials (Table S1). It is also found that the feeding Fe:Co molar ratio in the precursor solutions is typically much higher than that of the resulting MOFs. For example, when the precursor contains the same amount of $CoCl_2$ and $FeCl_2$, the resulting product has an Fe content as low as 5.29% (MOF **3** in Table 1). Even when $FeCl_2$ was 1000 times more than $CoCl_2$ in the precursor, Fe still makes up only 76.1% of the total metal centers in the product (MOF **1** in Table 1). When the precursor solution contains $FeCl_2$ and $CoCl_2$ in the 100:1 ratio, the resulting product has an Fe content of 46.1% (MOF **2** in Table 1). These results suggest that the incorporation rate of Fe into the framework is much slower compared to that of Co. During synthesis, the slower growth of the **FeTHT** framework was visually observed.

Table 1. Metal content in mixed-metal THT-based MOFs

Material	Feeding Fe:Co Molar Ratio	Average Product Fe:Co Molar Ratio	Average Fe%
1	1000	3.19 ± 0.04	76.1%
2	100	$(8.54 \pm 0.97) \times 10^{-1}$	46.1%
3	1	$(5.61 \pm 0.47) \times 10^{-2}$	5.29%

Powder X-ray diffraction (PXRD) measurements confirm the crystalline structure of the as-synthesized series of THT-based MOFs (Figure 1a). MOFs **1**, **2**, and **3** exhibit very similar PXRD patterns, with prominent peaks at 1.2°, 2.4°, 3.2° and 4.2°, indicating a similar crystalline structure regardless of the metal compositions. The PXRD patterns of the mixed-metal MOFs (**CoFeTHT**) also match with those of the Co and Fe-only MOFs, as well as with their simulated PXRD patterns. To confirm the structural similarity of the MOF series, FTIR spectrum was acquired for each MOF and compared to the simulated spectrum of a cobalt dithiolene molecular model (see SI for details). As shown in Figure S17, each MOF displays a very similar FTIR pattern and also shows relatively good agreement with the calculated spectrum. The only notable difference between the experimental and computational result is for the C–H stretching modes, which are experimentally observed at 2970–2870 cm^{-1}, but are calculated to be at 3150–3020 cm^{-1}. This is likely due to the discrepancy between the simulation model and the actual extended structure, which is discussed in detail in the SI. While the molecular model also influences the exact peak positions of the remainder of the spectrum, the number of peaks and relative positions allows for assignment of the spectrum as follows. The peaks at 1600–1300 cm^{-1} correspond to C–C bond stretches, the peaks at 1170–970 cm^{-1} correspond to C–H in-plane bending, the peaks at 925–800 cm^{-1} correspond to C–H out-of-plane bending, and the peaks at 680–525 cm^{-1} correspond to C–C out-of-plane bending. Finally, the S–H bond stretches at around 2520 cm^{-1} observed in the experimental spectra is likely caused by the residual unreacted THT ligand in the sample.

The chemical composition of the materials was further probed by X-ray photoelectron spectroscopy (XPS), which indicates the presence of Fe, Co, S, and C. The peak characteristics of each element appear similar for materials across the series, yet with variable peak intensities (Figure S1). Hence, **2** will be used herein as a representative example for discussions of the XPS features (Figures 1b, 1c). Two sets of peaks are observed in the Co 2p region, with binding energies of ~779 eV and ~794 eV. Deconvolution of these signals generates 5 peaks. The peaks at 779.8 and 794.8 eV are assigned to Co^{III}, the peaks at 778.6 and 793.6 eV are assigned to Co^{II}, and the broad peak at 782.2 eV is assigned to the Fe LMM Auger peak generated by the Al Kα source. For the Fe 2p regions, deconvolution of the signals at ~708 eV and ~721 eV also gives rise to a mixed valency of Fe^{II}/Fe^{III}, and the interference of the Co Auger peak (~713.2 eV) is again present. Excluding the Auger peaks, the characteristics of the Co and Fe regions are similar to those reported for materials with solely Co or Fe as the metal center, suggesting similar coordination environments.[5,36] The Co 2p region of **CoTHT** displays a set of broad peaks at around 779 and 794 eV, corresponding to the mixed-oxidation states of $Co^{II/III}$ induced by the non-innocent nature of the dithiolene ligands.[5] On the other hand, the Fe 2p region of **FeTHT** also shows a broad set of peaks around 708 eV and 721 eV, again fitted to the mixed-valency of $Fe^{II/III}$.[36] There-

fore, the similarities between the XPS results of the mixed-metal MOFs and the Co and Fe only MOFs further confirm that both metals are incorporated into the framework structure with the expected coordination environment.

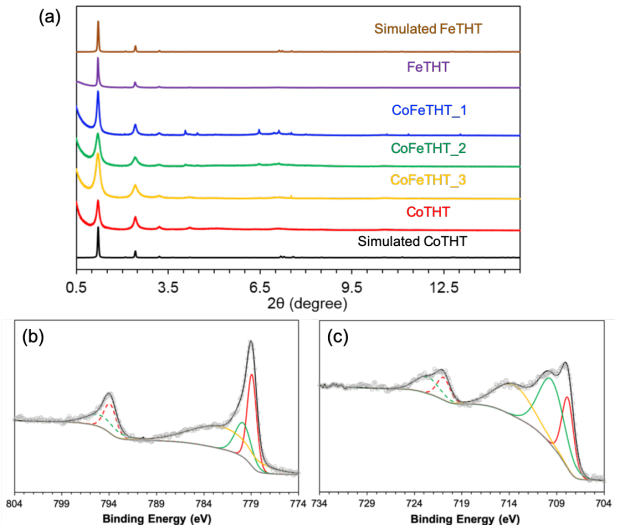

Figure 1. (a) Synchrotron and simulated PXRD patterns of THT-based MOFs, X-ray wavelength: 0.4127 Å. High-resolution XPS spectra of **2**: (b) Co 2p core level; (c) Fe 2p core level.

The morphology of the materials was evaluated by scanning electron-microscopy (SEM). As shown in Figure S2, materials with different metal ratios all display a sheet-like morphology, consistent with the previous reports on **CoTHT** and **FeTHT**.[5,37] The energy-dispersive X-ray spectroscopy (EDX) of **2** reveals the uniform distribution of Co, Fe, and S throughout the material (Figure S3), further confirming the chemical composition.

Electrocatalytic H_2 Evolution Studies. The electrocatalytic HER performance of **FeTHT** was first investigated by linear sweep voltammetry (LSV) in N_2-saturated pH 1.3 H_2SO_4 aqueous solutions using a three-electrode configuration (see SI for experimental details). In contrast to its cobalt counterpart, **FeTHT** displays poor electrocatalytic HER activity within the investigated electrochemical window (Figure S4a). A catalytic onset is seen at -0.440 V versus RHE and at large overpotentials (η > 0.70 V) the maximum current density achieved is only 3.5 mA·cm^{-2}, far less than the benchmarking metric of 10 mA·cm^{-2} for the HER. This poor performance is related to the large charge transfer resistance (R_{ct}) obtained by fitting the electrochemical impedance spectroscopy (EIS) data with the two-time constant serial (2TS) model (Figure S5). Although R_{ct} decreases at larger overpotentials (Table S2) as expected for an enhanced HER rate with increased catalytic driving force, the large R_{ct} at -0.518 V versus RHE (R_{ct} = 923 Ω) is still too prohibitive to allow for efficient catalysis. Sluggish charge transfer kinetics in the electrochemical window investigated thus precludes the ability to achieve high electrocatalytic activity. Tafel analysis reveals a Tafel slope of 210 mV/dec for **FeTHT** (Figure S4b), suggesting a large energy barrier for the rate-limiting Volmer-like discharge reaction.[46]

In addition to the low initial electrocatalytic activity, successive cyclic voltammetry (CV) experiments of **FeTHT** in a pH 1.3 solution revealed an unstable current response (Figure S6). A predominant irreversible redox wave is observed around 0 V versus RHE in the first cathodic sweep of the CV. During sequential scans, this feature gradually diminishes, shifting to more anodic potentials, and eventually disappearing. This behavior suggests a possible change in the electronic properties of the material under electrochemical polarization. Controlled potential electrolysis (CPE) experiments were performed to further evaluate the stability and H_2 production efficiency of **FeTHT**. As shown in Figure S7a, the current response is relatively stable yet extremely low (~0.5 mA) even under a large overpotential input (η = 0.518 V). This behavior further testifies the low activity of the catalyst as observed in the LSV studies (Figure S4). The Faradaic efficiency (FE) for H_2 production is quantified to be 72.2 ± 1.4%, suggesting more than a quarter of the electrons were consumed in other alternative Faradaic processes, likely related to the changing redox features observed in the CV studies (Figure S6). The EIS measurements reveal a drastic increase in the R_{ct} after CPE (Figure S7b, Table S3), indicating a much hindered HER kinetics after polarization. In view of the poor electrocatalytic activity and cyclability of **FeTHT**, attention was then turned to the electrochemical study of the mixed-metal MOFs, with the hypothesis that the inactive Fe sites could serve as the structural building blocks to dilute the Co sites and enhance the activity on a per-Co basis, similar to the report by Chang and coworkers.[29]

The HER activity of the mixed-metal MOFs **1**-**3** was first evaluated in pH 1.3 aqueous solutions using LSV. As shown in Figure 2a, upon increasing the Co content within the framework, the overall activity is substantially enhanced, with **3** exhibiting the highest activity for the mixed-metals MOFs. The catalytic onset is reduced from -0.440 V for **FeTHT** to -0.091 V for **3** and the Tafel slope is lowered from 210 mV/dec for **FeTHT** to 80.2 mV/dec for **3** (characteristic values summarized in Table 2). Such enhancement in activity correlates positively with the diminished R_{ct} value and enhanced double layer capacitance (C_{dl}) extracted from the EIS measurements (Figure S8). For **1**, the R_{ct} is as high as 4190 Ω even at η = 368 mV, whereas for **3** the R_{ct} is only 46.8 Ω at η = 168 mV. The C_{dl} values are used as an indicator of the electrocatalytically active surface area, and are extrapolated from the EIS spectra instead of cyclic voltammograms to obtain a more accurate description of the catalyst under the HER conditions.[47] The much larger C_{dl} value (15.9 mF) for **3** compared to 1.12 mF for **1** indicates the increase in Co content gives rise to a larger electrochemically active surface area (Table S4), suggesting Co metal center to be the actual catalytically active site. However, upon normalizing the current by the bulk loading of Co, **2** and **3** display similar activity that is much higher than the activity of **1**, and on par with that of the **CoTHT** (Figure 2b). This result was unanticipated, as one would expect that by diluting the electroactive Co sites with catalytically inert Fe sites, the activity would be boosted on a per-cobalt basis, as was reported for the multivariate Co/Cu COF-367 catalysts mentioned previously.[29] The experimental results observed herein suggest that, instead of being an inert site and serving merely as a diluting factor, the Fe site is playing a detrimental role and adversely influencing the overall activity at high concentrations.

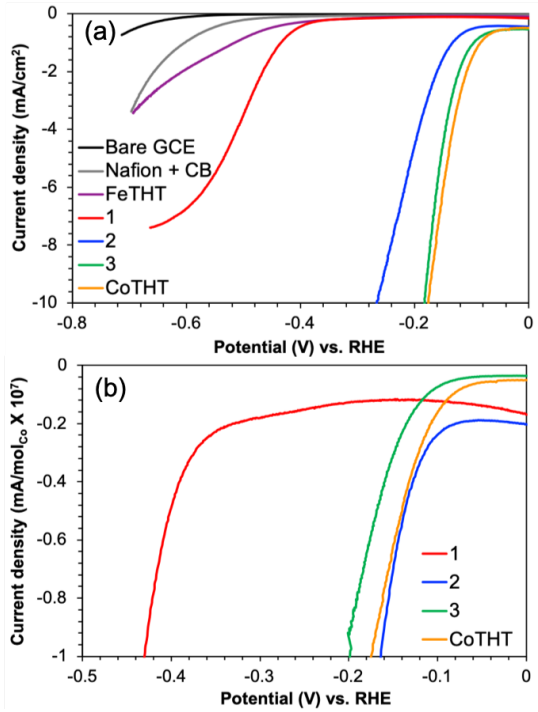

Figure 2. Polarization curves of **FeTHT**, mixed-metal MOF **1-3**, and **CoTHT** with current normalized by (a) geometric surface area and (b) bulk loading of the Co metal centers. All measurements were performed in N_2-saturated pH 1.3 aqueous solutions, scan rate: 5 mV/s, rotation rate: 2000 rpm. The non-zero background current is due to the non-Faradaic capacitive charging.

Table 2. Electrocatalytic properties of THT-based MOFs[a]

Material	Onset (V) vs. RHE	Tafel Slope (mV/dec)[b]
FeTHT	-0.440	210
1	-0.400	101
2	-0.117	95.2
3	-0.091	80.2
CoTHT	-0.079	81.6

a. See Table S7 for the HER activity comparison with other dithiolene-based electrocatalysts and Figure S16 for comparison with Pt/C; b. See Figure S9 for Tafel plots.

To further investigate the stability and HER performance of the mixed-metal MOFs, CPE experiments were performed. Figure 3 shows the current response of all three materials during a one hour electrolysis experiment at an overpotential of 0.418 V. MOF **1** exhibits a relatively stable, yet low current response (~ 0.1 mA), whereas **3** is able to maintain a relatively high current (~ 8 mA) over the period of one hour. The most interesting behavior is observed for **2**, where the current starts off high (~ 5 mA), but gradually declines over time (~ 1.6 mA at 60 min). The EIS measurements of **2** before and after electrolysis reveal a drastic increase in R_{ct} from 98.5 Ω to 940 Ω and a substantial decrease in C_{dl} from 19.3 mF to 4.25 mF (measured at η = 168 mV, Figure S10, Table S5). The changes in R_{ct} and C_{dl} suggest that the decline in activity is a result of the impeded charge transfer processes along with the diminished electrocatalytically active surface area. The ICP-OES analysis of the post-CPE electrolyte solutions revealed that the amount of Co and Fe in the solution is negligible, suggesting the diminished activity was not caused by the dissolution of the catalyst. Additionally, the Faradaic efficiency (FE) for H_2 generation for **1**, **2**, and **3** are 70.3%, 72.8%, and 86.6%, respectively, whereas **CoTHT** has a near unity FE for H_2 production as reported previously.[4,5] The extend of reduction in the FE correlates with the amount of Fe present in the framework, indicating that the **FeTHT** domains within the framework are going through alternative faradaic processes during electrolysis. The turnover frequency (TOF) of the catalysts was estimated by dividing the amount of H_2 produced (in moles) during the 1 hour CPE experiment by the catalyst loading (in moles of metals) determined by ICP-OES (Table S6). It is noteworthy that the as-calculated TOF is a lower-bound estimation of the actual TOF, as not all metal sites are electrochemically accessible and therefore, active, during electrolysis. If we assume only Co is responsible for catalysis, the corresponding TOF_{Co} is 11.8 h^{-1}, 85.7 h^{-1}, and 132 h^{-1} for **1**, **2**, and **3**, respectively (Table S6). These results demonstrate that the TOF_{Co} decreases drastically when more Fe is present in the catalyst, further suggesting that Fe is inhibiting the catalytic activity of the Co sites.

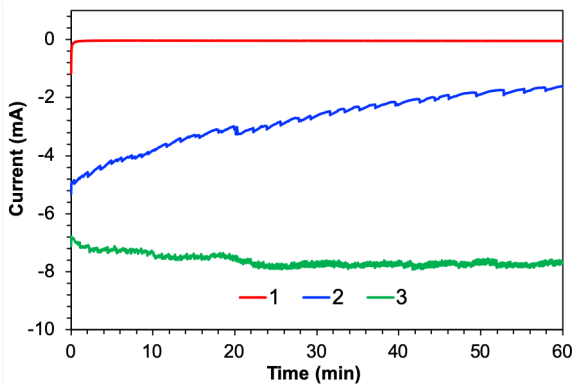

Figure 3. Controlled potential electrolysis (CPE) of **1** (red), **2** (blue), and **3** (green) at -0.418 V versus RHE in N_2-saturated pH 1.3 aqueous solutions.

The poor stability of the mixed-metal MOFs is also revealed by the CV studies in pH 10 electrolyte solutions. As shown in Figure S11b, when **1** is subjected to consecutive CV scans, the intensity of the redox feature centered around -0.3 V versus RHE diminishes gradually. The instability of the redox wave is also observed for **2** and **3**, albeit less drastic within the CV timescale in comparison to **1**. The **CoTHT** framework displays redox feature at similar potential, yet with better cyclability (Figure S12). The correlation between the extent of reduction in the redox feature and the content of Fe within the framework again suggests that the Fe domain is responsible for the instability of the material under electrochemical conditions.

Physical characterizations were performed on **FeTHT** and MOF **2** after electrolysis to provide insights into the electrochemical deactivation of the material. For **2**, the PXRD pattern taken after 1 hour CPE experiment shows a drastically diminished peak intensity at 4.5° and 9.1°, corresponding to the [100] and [200] reflection, respectively (Figure S13a). In the case of **FeTHT**, the intensity of these two peaks further diminishes to essentially an undetectable level (Figure S13b). The change in PXRD patterns suggests that the electrolysis leads to a deteriorated coherence within the 2D sheets, which is likely induced by the **FeTHT** domains, as the Co-only analogue is

capable of maintaining its structural integrity based on our previous study.[4] To detect the origin of the structural changes, XPS measurements were applied to elucidate the chemical environment after electrolysis. As shown in Figure S14a, the Fe 2p region of the post-CPE **FeTHT** displays a very broad peak ranging from 702 eV to 727 eV, suggesting the formation of new bonding environments of Fe centers. Additionally, a new satellite peak appears at around 233 eV in the S 2s region (Figure S14b), which could be contributed by the sulfonic acid group in the Nafion, though the possibility of a modified S environment in the dithiolene linker cannot be excluded. For post-CPE analysis of MOF **2**, the Fe 2p and S 2s regions display similar behaviors compared to those of **FeTHT** (Figure S15). The Co 2p peaks are present but hard to distinguish, because of the sloped baseline of the region, which is likely resulted from the interference of the Fe Auger series. Nevertheless, previous work with the Co-only analogue has suggested that electrolysis does not alter the Co 2p XPS features.[4] In short, the XPS characterizations indicate the transformation of the bonding environment for Fe, and possibly S for **FeTHT** and MOF **2**.

Discussion. Based on previous reports on molecular metal dithiolene complexes, **FeTHT** is expected to be an inferior electrocatalyst for the HER compared to **CoTHT**. Computational studies focused on the electronic structure of $[Fe(bdt)_2]$ and $[Co(bdt)_2]$ (bdt = benzene-1,2-dithiolate) molecular complexes have suggested that there are significant differences in the composition of the frontier orbitals. For $[Co(bdt)_2]$, the frontier orbitals possess mixed metal-ligand character (non-innocent), yet for $[Fe(bdt)_2]$, these orbitals are predominantly metal-centered.[48] Therefore, the dithiolate ligands in the $[Fe(bdt)_2]$ complex are considered innocent. Eisenberg and coworkers have illustrated that $[Fe(bdt)_2]$ has a more negative reduction potential (-0.90 V vs. SCE) compared to $[Co(bdt)_2]$ (-0.64 V vs. SCE), and exhibits lower activity when incorporated into a photocatalytic HER system.[35,49] The diminished HER activity of iron dithiolene complexes is expected to be retained upon incorporation into the extended THT-based framework. However, the extent of the reduction in the HER activity for **FeTHT** in comparison to **CoTHT** is much greater than anticipated. For the molecular $[Fe(bdt)_2]$ complex, although its activity is inferior compared to the Co analogue, it is still capable of performing photocatalytic HER for up to 80 hours with high turnover numbers.[35] Additionally, our previous study regarding an analogous polymer, **FeBHT**, where iron dithiolene active units are incorporated into an extended framework using BHT as linkers, has shown moderate activity towards the HER with a Tafel slope of 119 mV/dec and an overpotential of 473 mV to reach 10 mA/cm^2.[8] However, in this study, the electrocatalytic testing of **FeTHT** shows a minimum activity and an inability to achieve the HER benchmarking metric of 10 $mA \cdot cm^{-2}$ within the investigated potential window, while **CoTHT** is reported to be among the most active MOF-based HER catalysts.[4] Such large performance gap between **CoTHT** and **FeTHT** is also surprising from a physical property point of view, as a recent report demonstrates that the room-temperature electrical conductivity of the as-prepared **FeTHT** is comparable to that of **CoTHT**,[36,37] suggesting that **FeTHT** should be sufficiently conductive to promote charge transport in the pristine oxidation state.

Electrochemical characterizations suggest that under catalytic conditions, the **FeTHT** domains undergo alternative Faradaic processes that alter its electrochemical behavior. First, the diminished redox feature observed in the consecutive CV scans of **FeTHT** (Figure S6) suggests that the material is dynamically changing under operating conditions and the electrons seem to be trapped within the framework. Second, the EIS response of **FeTHT** reveals a much larger R_{ct} after 1 hour CPE experiment (Figure S7), indicating a more hindered HER kinetics on the post-CPE catalyst, or in other words, the material becomes less active during electrolysis. The electrochemical instability of **FeTHT** persists within the mixed-metal frameworks. For instance, the CV studies of the mixed-metal MOFs in pH 10 electrolyte solutions highlight the limited cyclability of the Fe-containing MOFs (Figure S11). Within the same timescale, the change in the redox feature is more drastic for **1** relative to **2** and **3**, indicating that when more Fe is present in the framework, the material is more prone to have altered electrochemical behaviors. Furthermore, the compromised FEs for Fe-containing MOFs demonstrate that electrons undergo alternative Faradaic processes other than the HER. It is observed that the loss of FE correlates positively with the increase in Fe content, indicating that the **FeTHT** domains are responsible for the loss of FE. Post-electrolysis physical characterizations of the catalysts suggest that the altered electrochemical behavior could be attributed to the changes in the local coordination geometry of the Fe center. The PXRD measurements of MOF **2** and **FeTHT** after electrochemical treatment display peaks with diminished intensity, indicating a deteriorated coherence within the 2D sheets (Figure S13). Additionally, the XPS features of the Fe 2p and S 2s regions are very different between the pristine and post-electrolysis catalysts, suggesting a change in the bonding environment of the Fe sites (Figures S14, S15).

In an attempt to lower the catalyst cost and enhance the activity on a per-site basis, a series of mixed Co/Fe MOFs were tested for the hydrogen evolution reaction. However, the polarization curves normalized on the cobalt loading (Figure 2b) suggest that the presence of Fe does not boost the activity of the Co sites. Furthermore, the CPE experiments (Figure 3) show that the presence of Fe can in fact suppress the performance of the Co sites. For **2**, where the metal composition is roughly 50% Co and 50% Fe, the current response drastically decreases over the course of the electrolysis, indicating that the high intrinsic activity of the Co sites are masked in the presence of Fe. The calculated average TOF of the MOFs (Table S6) also illustrates that when more Fe is present in the framework, the Co sites appear to behave less active for the HER.

To explain the adverse impact of Fe sites on the HER activity of the mixed-metal frameworks, it is proposed that the electrochemical treatment of **FeTHT** yields a material with attenuated charge transfer ability, rendering the originally active Co sites inaccessible by the electrons. This conductivity-switching phenomenon has been observed by Boettcher and coworkers while studying transition metal oxyhydroxides for electrocatalytic OER.[44,45,50] The electrical conductivity of the oxyhydroxides is found to be higher under anodic potentials and lower under cathodic potentials. Although similar behavior has not been reported for any THT-based materials, it has been seen in some analogous BHT-based materials. For example, the NiBHT and AgBHT frameworks are found to exhibit a lower electrical conductivity upon chemical reduction.[51,52] These prior studies, together with the electrochemical behavior of **FeTHT** observed in this work, suggest the possibility of a declined electron transfer ability of **FeTHT** under electrocata-

lytic conditions, which could be caused by the change in the coordination geometry of the Fe sites.

For example, it is possible that the diminished redox feature observed for **FeTHT** is due to the low ability of the reduced **FeTHT** to undergo electron transfer, which essentially forms an insulating layer at the electrode/catalyst interface that prevents further electronic communication. Additionally, the large Tafel slope of **FeTHT** (210 mV/dec) indicates a large kinetic barrier for the first one-electron one-proton reduction (Volmer step), which could arise from the insulating nature of the reduced **FeTHT**. Upon incorporation of Co, which is known to be active under cathodic potentials, the energy barrier for electron transfer is lowered, leading to a decrease in Tafel slope (Table 2). Following the same line, the deactivation mechanism of the mixed-metal MOFs can also be rationalized. During electrolysis, the **FeTHT** domains would be reduced and deactivated gradually. As these **FeTHT** domains are distributed homogeneously throughout the framework, as suggested by the EDX mapping, their deactivation can impede electron transfer within the entire structure, rendering the active Co sites catalytically inert. This aligns well with the changes in the R_{ct} and C_{dl} values of MOF **2** observed after 1 hour of electrolysis (Table S5); the almost 10 fold increase in R_{ct} suggests a severely hindered charge transfer kinetics, whereas the drastically decreased C_{dl} reveals a diminished number of the catalytically active sites. When more Fe is present in the framework, the deactivation process is accelerated, which is observed in the more pronounced deactivating behavior of **2** in comparison to **3**. As for **1**, due to the significantly higher Fe concentration within the structure, the material deactivates rapidly and exhibits electrocatalytic activity analogous to that of **FeTHT**.

CONCLUSIONS

In summary, taking advantage of the synthetic tunability of MOFs, a series of THT-based MOFs with varying stoichiometries of cobalt and iron were synthesized and characterized. The composition of the materials can be readily altered by tuning the ratios of the iron and cobalt precursors, as revealed by ICP-OES and confirmed by XPS and EDX measurements. The materials within the series possess similar crystalline structures regardless of the chemical composition, as suggested by PXRD and FTIR measurements. The electrocatalytic HER activities of the materials were characterized in pH 1.3 aqueous solutions. It is found that, unlike its Co analogue, **FeTHT** exhibits minimal activity towards the HER, with a catalytic onset of -0.440 V versus RHE and a Tafel slope of 210 mV/dec. Upon incorporation of more Co into the framework, the overall electrocatalytic HER activity of the framework increases drastically, indicating Co being the catalytically active center. However, further investigation suggests that Fe centers within the framework are not merely inert spectator species serving to dilute the catalytically active Co centers, but rather active inhibitors of efficient and steady H_2 evolution. The long-term stability of the material as well as the FE for H_2 production drastically decline when more Fe is present in the structure. Post-electrolysis characterizations of the catalysts suggest a diminished crystallinity and a drastically altered chemical environment for the Fe sites. It is proposed that the poor activity of **FeTHT** and the adverse effect of the Fe centers in the mixed-metal frameworks originate from the ability of iron-containing materials to participate in alternative Faradaic processes, leading to a material that is less electrochemically active for the HER. This hypothesis is supported by EIS characterizations and CV studies where an irreversible redox peak is observed to diminish over consecutive CV scans. Future experimental studies such as in-situ conductivity measurements and X-ray absorption spectroscopy measurements, as well as density functional theory calculations are necessary to fully elucidate the deactivation mechanism of the Fe and mixed-metal MOFs. Our work suggests that, while incorporating tunable molecular units into extended frameworks serves as an attractive strategy to build heterogeneous electrocatalysts, precautions should be taken when carrying out this strategy, as the physical properties of the bulk material, such as the ability to move charge, could be altered under catalytic conditions and adversely impact the overall activity of the material. Furthermore, although diluting expensive, highly active metals with cheaper, more abundant, and catalytically inert metals is a method to increase the per-site activity and decrease the overall cost of the catalyst, our observation of the decrease in activity of the Co active sites with increasing Fe content demonstrates that the identity of the diluting metal should be chosen carefully.

ASSOCIATED CONTENT

Supporting Information

The Supporting Information is available free of charge on the ACS Publications website.
Experimental methods, Table S1-S7, and Figure S1-S17 (PDF)

AUTHOR INFORMATION

Corresponding Author

* E-mail: smarines@usc.edu

Notes

The authors declare no competing financial interest.

Notes

Any additional relevant notes should be placed here.

ACKNOWLEDGMENT

The research was primarily supported by the U. S. Department of Energy, Office of Basic Energy Sciences, Division of Chemical Sciences, Geosciences and Biosciences under Award DE-SC0019236. Additional support was provided by the National Science Foundation under award DMR-2004868 (FTIR experimental studies) and by the U. S. Department of Energy, Office of Basic Energy Sciences, Division of Chemical Sciences, Geosciences and Biosciences under Award DE-FG02-17ER16362 (FTIR theoretical studies). KC gratefully acknowledges the University of Southern California (USC) Wrigley Institute for the Norma and Jerol Sonosky summer fellowship. Use of the Advanced Photon Source at Argonne National Laboratory was supported by the U. S. Department of Energy, Office of Science, Office of Basic Energy Sciences, under Contract No. DE-AC02-06CH11357. XPS and SEM data were collected at the Core Center of Excellence in Nano Imaging, USC. We thank Dr. Andrew J. Clough for assistance with the collection of the SEM images. JDG acknowledges the Minnesota Supercomputing Institute (MSI) at the University of Minnesota and the National Energy Research Scientific Computing Center (NERSC), a DOE Office of Science User Facility supported by the Office of Science of the U.S. Department of

Energy under Contract No. DE-AC02-05CH11231, for providing resources that contributed to the computational results reported within this paper.

REFERENCES

(1) Zhou, H. C.; Long, J. R.; Yaghi, O. M. Introduction to Metal-Organic Frameworks. *Chem. Rev.* **2012**, *112* (2), 673–674.

(2) Downes Courtney, A.; Marinescu Smaranda, C. Electrocatalytic Metal–Organic Frameworks for Energy Applications. *ChemSusChem* **2017**, *10* (22), 4374–4392.

(3) Drake, T.; Ji, P.; Lin, W. Site Isolation in Metal-Organic Frameworks Enables Novel Transition Metal Catalysis. *Acc. Chem. Res.* **2018**, *51* (9), 2129–2138.

(4) Chen, K.; Downes, C. A.; Schneider, E.; Goodpaster, J. D.; Marinescu, S. C. Improving and Understanding the Hydrogen Evolving Activity of a Cobalt Dithiolene Metal–Organic Framework. *ACS Appl. Mater. Interfaces* **2021**, *13* (14), 16384–16395.

(5) Clough, A. J.; Yoo, J. W.; Mecklenburg, M. H.; Marinescu, S. C. Two-Dimensional Metal–Organic Surfaces for Efficient Hydrogen Evolution from Water. *J. Am. Chem. Soc.* **2015**, *137* (1), 118–121.

(6) Sun, X.; Wu, K.-H.; Sakamoto, R.; Kusamoto, T.; Maeda, H.; Ni, X.; Jiang, W.; Liu, F.; Sasaki, S.; Masunaga, H.; Nishihara, H. Bis(Aminothiolato)Nickel Nanosheet as a Redox Switch for Conductivity and an Electrocatalyst for the Hydrogen Evolution Reaction. *Chem. Sci.* **2017**, *8* (12), 8078–8085.

(7) Dong, R.; Zheng, Z.; Tranca, D. C.; Zhang, J.; Chandrasekhar, N.; Liu, S.; Zhuang, X.; Seifert, G.; Feng, X. Immobilizing Molecular Metal Dithiolene-Diamine Complexes on 2D Metal-Organic Frameworks for Electrocatalytic H_2 Production. *Chem. Eur. J.* **2017**, *23* (10), 2255–2260.

(8) Downes, C. A.; Clough, A. J.; Chen, K.; Yoo, J. W.; Marinescu, S. C. Evaluation of the H_2 Evolving Activity of Benzenehexathiolate Coordination Frameworks and the Effect of Film Thickness on H_2 Production. *ACS Appl. Mater. Interfaces* **2018**, *10* (2), 1719–1727.

(9) Dong, R.; Pfeffermann, M.; Liang, H.; Zheng, Z.; Zhu, X.; Zhang, J.; Feng, X. Large-Area, Free-Standing, Two-Dimensional Supramolecular Polymer Single-Layer Sheets for Highly Efficient Electrocatalytic Hydrogen Evolution. *Angew. Chem. Int. Ed.* **2015**, *54* (41), 12058–12063.

(10) Qin, J.-S.; Du, D.-Y.; Guan, W.; Bo, X.-J.; Li, Y.-F.; Guo, L.-P.; Su, Z.-M.; Wang, Y.-Y.; Lan, Y.-Q.; Zhou, H.-C. Ultrastable Polymolybdate-Based Metal–Organic Frameworks as Highly Active Electrocatalysts for Hydrogen Generation from Water. *J. Am. Chem. Soc.* **2015**, *137* (22), 7169–7177.

(11) Hod, I.; Deria, P.; Bury, W.; Mondloch, J. E.; Kung, C.-W.; So, M.; Sampson, M. D.; Peters, A. W.; Kubiak, C. P.; Farha, O. K.; Hupp, J. T. A Porous Proton-Relaying Metal-Organic Framework Material That Accelerates Electrochemical Hydrogen Evolution. *Nat. Commun.* **2015**, *6* (1), 8304.

(12) Wu, Y.-P.; Zhou, W.; Zhao, J.; Dong, W.-W.; Lan, Y.-Q.; Li, D.-S.; Sun, C.; Bu, X. Surfactant-Assisted Phase-Selective Synthesis of New Cobalt MOFs and Their Efficient Electrocatalytic Hydrogen Evolution Reaction. *Angew. Chem. Int. Ed.* **2017**, *56* (42), 13001–13005.

(13) Micheroni, D.; Lan, G.; Lin, W. Efficient Electrocatalytic Proton Reduction with Carbon Nanotube-Supported Metal–Organic Frameworks. *J. Am. Chem. Soc.* **2018**, *140* (46), 15591–15595.

(14) Huang, X.; Yao, H.; Cui, Y.; Hao, W.; Zhu, J.; Xu, W.; Zhu, D. Conductive Copper Benzenehexathiol Coordination Polymer as a Hydrogen Evolution Catalyst. *ACS Appl. Mater. Interfaces* **2017**, *9* (46), 40752–40759.

(15) Gong, Y.; Shi, H.-F.; Hao, Z.; Sun, J.-L.; Lin, J.-H. Two Novel Co(II) Coordination Polymers Based on 1,4-Bis(3-Pyridylaminomethyl)Benzene as Electrocatalysts for Oxygen Evolution from Water. *Dalt. Trans.* **2013**, *42* (34), 12252-12259.

(16) Kung, C.-W.; Mondloch, J. E.; Wang, T. C.; Bury, W.; Hoffeditz, W.; Klahr, B. M.; Klet, R. C.; Pellin, M. J.; Farha, O. K.; Hupp, J. T. Metal–Organic Framework Thin Films as Platforms for Atomic Layer Deposition of Cobalt Ions To Enable Electrocatalytic Water Oxidation. *ACS Appl. Mater. Interfaces* **2015**, *7* (51), 28223–28230.

(17) Lu, X. F.; Liao, P. Q.; Wang, J. W.; Wu, J. X.; Chen, X. W.; He, C. T.; Zhang, J. P.; Li, G. R.; Chen, X. M. An Alkaline-Stable, Metal Hydroxide Mimicking Metal-Organic Framework for Efficient Electrocatalytic Oxygen Evolution. *J. Am. Chem. Soc.* **2016**, *138* (27), 8336–8339.

(18) Johnson, B. A.; Bhunia, A.; Ott, S. Electrocatalytic Water Oxidation by a Molecular Catalyst Incorporated into a Metal–Organic Framework Thin Film. *Dalt. Trans.* **2017**, *46* (5), 1382–1388.

(19) Lin, S.; Pineda-Galvan, Y.; Maza, W. A.; Epley, C. C.; Zhu, J.; Kessinger, M. C.; Pushkar, Y.; Morris, A. J. Electrochemical Water Oxidation by a Catalyst-Modified Metal-Organic Framework Thin Film. *ChemSusChem* **2017**, *10* (3), 514–522.

(20) Shen, J.-Q.; Liao, P.-Q.; Zhou, D.-D.; He, C.-T.; Wu, J.-X.; Zhang, W.-X.; Zhang, J.-P.; Chen, X.-M. Modular and Stepwise Synthesis of a Hybrid Metal–Organic Framework for Efficient Electrocatalytic Oxygen Evolution. *J. Am. Chem. Soc.* **2017**, *139* (5), 1778–1781.

(21) Miner, E. M.; Fukushima, T.; Sheberla, D.; Sun, L.; Surendranath, Y.; Dincă, M. Electrochemical Oxygen Reduction Catalysed by Ni_3(Hexaiminotriphenylene)$_2$. *Nat. Commun.* **2016**, *7* (1), 10942.

(22) Miner, E. M.; Gul, S.; Ricke, N. D.; Pastor, E.; Yano, J.; Yachandra, V. K.; Van Voorhis, T.; Dincă, M. Mechanistic Evidence for Ligand-Centered Electrocatalytic Oxygen Reduction with the Conductive MOF Ni_3(Hexaiminotriphenylene)$_2$. *ACS Catal.* **2017**, *7* (11), 7726–7731.

(23) Miner, E. M.; Wang, L.; Dincă, M. Modular O_2 Electroreduction Activity in Triphenylene-Based Metal–Organic Frameworks. *Chem. Sci.* **2018**, *9* (29), 6286–6291.

(24) Usov, P. M.; Huffman, B.; Epley, C. C.; Kessinger, M. C.; Zhu, J.; Maza, W. A.; Morris, A. J. Study of Electrocatalytic Properties of Metal–Organic Framework PCN-223 for the Oxygen Reduction Reaction. *ACS Appl. Mater. Interfaces* **2017**, *9* (39), 33539–33543.

(25) Lions, M.; Tommasino, J.-B.; Chattot, R.; Abeykoon, B.; Guillou, N.; Devic, T.; Demessence, A.; Cardenas, L.; Maillard, F.; Fateeva, A. Insights into the Mechanism of Electrocatalysis of the Oxygen Reduction Reaction by a Porphyrinic Metal Organic Framework. *Chem. Commun.* **2017**, *53* (48), 6496–6499.

(26) Liu, X. H.; Hu, W. L.; Jiang, W. J.; Yang, Y. W.; Niu, S.; Sun, B.; Wu, J.; Hu, J. S. Well-Defined Metal-O_6 in Metal-Catecholates as a Novel Active Site for Oxygen Electroreduction. *ACS Appl. Mater. Interfaces* **2017**, *9* (34), 28473–28477.

(27) Kornienko, N.; Zhao, Y.; Kley, C. S.; Zhu, C.; Kim, D.; Lin, S.; Chang, C. J.; Yaghi, O. M.; Yang, P. Metal–Organic Frameworks for Electrocatalytic Reduction of Carbon Dioxide. *J. Am. Chem. Soc.* **2015**, *137* (44), 14129–14135.

(28) Hod, I.; Sampson, M. D.; Deria, P.; Kubiak, C. P.; Farha, O. K.; Hupp, J. T. Fe-Porphyrin-Based Metal–Organic Framework Films as High-Surface Concentration, Heterogeneous Catalysts for Electrochemical Reduction of CO_2. *ACS Catal.* **2015**, *5* (11), 6302–6309.

(29) Lin, S.; Diercks, C. S.; Zhang, Y.-B.; Kornienko, N.; Nichols, E. M.; Zhao, Y.; Paris, A. R.; Kim, D.; Yang, P.; Yaghi, O. M.; Chang, C. J. Covalent Organic Frameworks Comprising Cobalt Porphyrins for Catalytic CO_2 Reduction in Water. *Science* **2015**, *349* (6253), 1208.

(30) Johnson, E. M.; Haiges, R.; Marinescu, S. C. Covalent-Organic Frameworks Composed of Rhenium Bipyridine and Metal Porphyrins: Designing Heterobimetallic Frameworks with Two Distinct Metal Sites. *ACS Appl. Mater. Interfaces* **2018**, *10* (44), 37919–37927.

(31) Meng, Z.; Luo, J.; Li, W.; Mirica, K. A. Hierarchical Tuning of the Performance of Electrochemical Carbon Dioxide Reduction Using Conductive Two-Dimensional Metallophthalocyanine Based Metal-Organic Frameworks. *J. Am. Chem. Soc.* **2020**, *142* (52), 21656–21669.

(32) Diercks, C. S.; Lin, S.; Kornienko, N.; Kapustin, E. A.; Nichols, E. M.; Zhu, C.; Zhao, Y.; Chang, C. J.; Yaghi, O. M. Reticular

Electronic Tuning of Porphyrin Active Sites in Covalent Organic Frameworks for Electrocatalytic Carbon Dioxide Reduction. *J. Am. Chem. Soc.* **2018**, *140* (3), 1116–1122.

(33) Matheu, R.; Gutierrez-Puebla, E.; Monge, M. Á.; Diercks, C. S.; Kang, J.; Prévot, M. S.; Pei, X.; Hanikel, N.; Zhang, B.; Yang, P.; Yaghi, O. M. Three-Dimensional Phthalocyanine Metal-Catecholates for High Electrochemical Carbon Dioxide Reduction. *J. Am. Chem. Soc.* **2019**, *141* (43), 17081–17085.

(34) Kusamoto, T.; Nishihara, H. Zero-, One- and Two-Dimensional Bis(Dithiolato)Metal Complexes with Unique Physical and Chemical Properties. *Coord. Chem. Rev.* **2019**, *380*, 419–439.

(35) Lv, H.; Ruberu, T. P. A.; Fleischauer, V. E.; Brennessel, W. W.; Neidig, M. L.; Eisenberg, R. Catalytic Light-Driven Generation of Hydrogen from Water by Iron Dithiolene Complexes. *J. Am. Chem. Soc.* **2016**, *138* (36), 11654–11663.

(36) Clough, A. J.; Orchanian, N. M.; Skelton, J. M.; Neer, A. J.; Howard, S. A.; Downes, C. A.; Piper, L. F. J.; Walsh, A.; Melot, B. C.; Marinescu, S. C. Room Temperature Metallic Conductivity in a Metal–Organic Framework Induced by Oxidation. *J. Am. Chem. Soc.* **2019**, *141* (41), 16323-16330.

(37) Clough, A. J.; Skelton, J. M.; Downes, C. A.; de la Rosa, A. A.; Yoo, J. W.; Walsh, A.; Melot, B. C.; Marinescu, S. C. Metallic Conductivity in a Two-Dimensional Cobalt Dithiolene Metal–Organic Framework. *J. Am. Chem. Soc.* **2017**, *139* (31), 10863–10867.

(38) Dong, R.; Han, P.; Arora, H.; Ballabio, M.; Karakus, M.; Zhang, Z.; Shekhar, C.; Adler, P.; Petkov, P. St.; Erbe, A.; Mannsfeld, S. C. B.; Felser, C.; Heine, T.; Bonn, M.; Feng, X.; Cánovas, E. High-Mobility Band-like Charge Transport in a Semiconducting Two-Dimensional Metal–Organic Framework. *Nat. Mater.* **2018**, *17* (11), 1027–1032.

(39) Deng, H.; Doonan, C. J.; Furukawa, H.; Ferreira, R. B.; Towne, J.; Knobler, C. B.; Wang, B.; Yaghi, O. M. Multiple Functional Groups of Varying Ratios in Metal-Organic Frameworks. *Science* **2010**, *327*, 846–850.

(40) Wang, L. J.; Deng, H.; Furukawa, H.; Gándara, F.; Cordova, K. E.; Peri, D.; Yaghi, O. M. Synthesis and Characterization of Metal-Organic Framework-74 Containing 2, 4, 6, 8, and 10 Different Metals. *Inorg. Chem.* **2014**, *53* (12), 5881–5883.

(41) Zhang, B.; Zheng, Y.; Ma, T.; Yang, C.; Peng, Y.; Zhou, Z.; Zhou, M.; Li, S.; Wang, Y.; Cheng, C. Designing MOF Nanoarchitectures for Electrochemical Water Splitting. *Adv. Mater.* **2021**, *33* (17), 2006042.

(42) Zhao, Q.; Lin, X.; Zhou, J.; Zhao, C.; Zheng, D.; Song, S.; Jing, C.; Zhang, L.; Wang, J. A Tunable Amorphous Heteronuclear Iron and Cobalt Imidazolate Framework Analogue for Efficient Oxygen Evolution Reactions. *Eur. J. Inorg. Chem.* **2021**, *2021* (8), 702–707.

(43) Dang, Y.; Han, P.; Li, Y.; Zhang, Y.; Zhou, Y. Low-Crystalline Mixed Fe-Co-MOFs for Efficient Oxygen Evolution Electrocatalysis. *J. Mater. Sci.* **2020**, *55* (28), 13951–13963.

(44) Burke, M. S.; Kast, M. G.; Trotochaud, L.; Smith, A. M.; Boettcher, S. W. Cobalt-Iron (Oxy)Hydroxide Oxygen Evolution Electrocatalysts: The Role of Structure and Composition on Activity, Stability, and Mechanism. *J. Am. Chem. Soc.* **2015**, *137* (10), 3638–3648.

(45) Batchellor, A. S.; Boettcher, S. W. Pulse-Electrodeposited Ni-Fe (Oxy)Hydroxide Oxygen Evolution Electrocatalysts with High Geometric and Intrinsic Activities at Large Mass Loadings. *ACS Catal.* **2015**, *5* (11), 6680–6689.

(46) Shinagawa, T.; Garcia-Esparza, A. T.; Takanabe, K. Insight on Tafel Slopes from a Microkinetic Analysis of Aqueous Electrocatalysis for Energy Conversion. *Sci. Rep.* **2015**, *5* (1), 13801.

(47) Downes, C. A.; Marinescu, S. C. Understanding Variability in the Hydrogen Evolution Activity of a Cobalt Anthracenetetrathiolate Coordination Polymer. *ACS Catal.* **2017**, *7* (12), 8605–8612.

(48) Ray, K.; Begum, A.; Weyhermüller, T.; Piligkos, S.; Van Slageren, J.; Neese, F.; Wieghardt, K. The Electronic Structure of the Isoelectronic, Square-Planar Complexes $[Fe^{II}(L)_2]^{2-}$ and $[Co^{III}(LBu)_2]^-$ (L^{2-} and $(LBu)_2^-$ = Benzene-1,2-Dithiolates): An Experimental and Density Functional Theoretical Study. *J. Am. Chem. Soc.* **2005**, *127* (12), 4403–4415.

(49) Das, A.; Han, Z.; Haghighi, M. G.; Eisenberg, R. Photogeneration of Hydrogen from Water Using CdSe Nanocrystals Demonstrating the Importance of Surface Exchange. *Proc. Natl. Acad. Sci.* **2013**, *110* (42), 16716–16723.

(50) Stevens, M. B.; Enman, L. J.; Batchellor, A. S.; Cosby, M. R.; Vise, A. E.; Trang, C. D. M.; Boettcher, S. W. Measurement Techniques for the Study of Thin Film Heterogeneous Water Oxidation Electrocatalysts. *Chem. Mater.* **2017**, *29* (1), 120–140.

(51) Kambe, T.; Sakamoto, R.; Hoshiko, K.; Takada, K.; Miyachi, M.; Ryu, J. H.; Sasaki, S.; Kim, J.; Nakazato, K.; Takata, M.; Nishihara, H. π-Conjugated Nickel Bis(Dithiolene) Complex Nanosheet. *J. Am. Chem. Soc.* **2013**, *135* (7), 2462–2465.

(52) Huang, X.; Li, H.; Tu, Z.; Liu, L.; Wu, X.; Chen, J.; Liang, Y.; Zou, Y.; Yi, Y.; Sun, J.; Xu, W.; Zhu, D. Highly Conducting Neutral Coordination Polymer with Infinite Two-Dimensional Silver–Sulfur Networks. *J. Am. Chem. Soc.* **2018**, *140* (45), 15153–15156.

Synopsis:

Two-dimensional dithiolene-based metal-organic frameworks (MOFs) are among the most active MOF-based electrocatalysts for the hydrogen evolution reaction. Herein, a series of MOFs with 2,3,6,7,10,11-triphenylenehexathiolate linkers and mixed cobalt and iron centers are synthesized and characterized by various spectroscopic techniques. The electrocatalytic performance of the MOFs suggests that the incorporation of the Fe centers adversely influences the expression of the high intrinsic activity of the Co centers, due to alternative Faradaic processes under catalytic conditions.

Table of Contents (TOC) graphic: